Springer

Dear Author,

Here are the proofs of your article.

- You can submit your corrections **online**, via **e-mail** or by **fax**.
- For **online** submission please insert your corrections in the online correction form. Always indicate the line number to which the correction refers.
- You can also insert your corrections in the proof PDF and **email** the annotated PDF.
- For fax submission, please ensure that your corrections are clearly legible. Use a fine black pen and write the correction in the margin, not too close to the edge of the page.
- Remember to note the **journal title**, **article number**, and **your name** when sending your response via e-mail or fax.
- **Check** the metadata sheet to make sure that the header information, especially author names and the corresponding affiliations are correctly shown.
- **Check** the questions that may have arisen during copy editing and insert your answers/ corrections.
- **Check** that the text is complete and that all figures, tables and their legends are included. Also check the accuracy of special characters, equations, and electronic supplementary material if applicable. If necessary refer to the *Edited manuscript*.
- The publication of inaccurate data such as dosages and units can have serious consequences. Please take particular care that all such details are correct.
- Please **do not** make changes that involve only matters of style. We have generally introduced forms that follow the journal's style.
  Substantial changes in content, e.g., new results, corrected values, title and authorship are not allowed without the approval of the responsible editor. In such a case, please contact the Editorial Office and return his/her consent together with the proof.
- If we do not receive your corrections **within 48 hours**, we will send you a reminder.
- Your article will be published **Online First** approximately one week after receipt of your corrected proofs. This is the **official first publication** citable with the DOI. **Further changes are, therefore, not possible.**
- The **printed version** will follow in a forthcoming issue.

Please note

After online publication, subscribers (personal/institutional) to this journal will have access to the complete article via the DOI using the URL: http://dx.doi.org/[DOI].
If you would like to know when your article has been published online, take advantage of our free alert service. For registration and further information go to: http://www.link.springer.com.

Due to the electronic nature of the procedure, the manuscript and the original figures will only be returned to you on special request. When you return your corrections, please inform us if you would like to have these documents returned.

Metadata of the article that will be visualized in OnlineFirst

ArticleTitle	Thermo-migration behavior of SAC305 lead-free solder reinforced with fullerene nanoparticles	
Article Sub-Title		
Article CopyRight	Springer Science+Business Media New York (This will be the copyright line in the final PDF)	
Journal Name	Journal of Materials Science	
Corresponding Author	Family Name	**Liu**
	Particle	
	Given Name	**Changqing**
	Suffix	
	Division	Wolfson School of Mechanical
	Organization	Electrical and Manufacturing Engineering, Loughborough University
	Address	Loughborough, UK
	Email	C.Liu@lboro.ac.uk
	ORCID	
Corresponding Author	Family Name	**Wu**
	Particle	
	Given Name	**Fengshun**
	Suffix	
	Division	State Key Laboratory of Materials Processing and Die and Mould Technology
	Organization	Huazhong University of Science and Technology
	Address	Wuhan, 430074, China
	Email	fengshunwu@hust.edu.cn
	ORCID	
Author	Family Name	**Chen**
	Particle	
	Given Name	**Guang**
	Suffix	
	Division	State Key Laboratory of Materials Processing and Die and Mould Technology
	Organization	Huazhong University of Science and Technology
	Address	Wuhan, 430074, China
	Division	Wolfson School of Mechanical
	Organization	Electrical and Manufacturing Engineering, Loughborough University
	Address	Loughborough, UK
	Email	
	ORCID	
Author	Family Name	**Liu**
	Particle	
	Given Name	**Li**
	Suffix	

	Division	Wolfson School of Mechanical
	Organization	Electrical and Manufacturing Engineering, Loughborough University
	Address	Loughborough, UK
	Email	
	ORCID	
Author	Family Name	**Du**
	Particle	
	Given Name	**Juan**
	Suffix	
	Division	Wolfson School of Mechanical
	Organization	Electrical and Manufacturing Engineering, Loughborough University
	Address	Loughborough, UK
	Email	
	ORCID	
Author	Family Name	**Silberschmidt**
	Particle	
	Given Name	**Vadim V.**
	Suffix	
	Division	Wolfson School of Mechanical
	Organization	Electrical and Manufacturing Engineering, Loughborough University
	Address	Loughborough, UK
	Email	
	ORCID	
Author	Family Name	**Chan**
	Particle	
	Given Name	**Y. C.**
	Suffix	
	Division	Department of Electronic Engineering
	Organization	City University of Hong Kong
	Address	Tat Chee Avenue, Kowloon Tong, Hong Kong
	Email	
	ORCID	

Schedule	Received	18 April 2016
	Revised	
	Accepted	18 July 2016

Abstract

In this work, SAC305 lead-free solder reinforced with 0.1 wt. % fullerene nanoparticles was prepared using a powder metallurgy method. A lab-made setup and a corresponding Cu/solder/Cu sample for thermo-migration (TM) test were designed and implemented. The feasibility of this setup for TM stressing was further verified with experimental and simulation methods; a temperature gradient in a solder seam was calculated as 1070 K/cm. Microstructural evolution and mechanical properties of both plain and composite solder alloys were then studied under the condition of TM stressing. It was shown that compared to unreinforced SAC305 solder, the process of diffusion of Cu atoms in the composite solder seam was remarkably suppressed. After the TM test for 600 h, Cu/solder interfaces in the composite solder seam were more stable and the inner structure remained more intact. Moreover, the addition of fullerene reinforcement can considerably affect a distribution of Cu_6Sn_5 formed as a result of dissolution of Cu atoms during the TM test. Hardness data across the solder seam were also found notably different because of the elemental redistribution caused by TM.

Footnote Information

_2D materials
_*ab initio* calculations
_additive manufacturing
_adhesion
_adsorption
_aerogels
_AFM
_alloys
_amorphous materials
_annealing
_antifouling materials
_atomic-layer deposition (ALD)
_atomistic modeling
_batteries
_batteries, lithium
_batteries, magnesium
_batteries, sodium
_BCC metals
_bio-inspired materials
_biomass conversion
_biomaterials
_biomechanics
_biomimetic
_black phosphorus
_blends
_brazing
_calcification
_capacitors
_carbon fiber
_carbon nanotube
_casting
_catalysts or catalysis
_cellular materials
_cellulose
_ceramics
_characterization methods
_chemical vapor deposition (CVD)
_CO_2 sequestration
_coatings
_colloids or bio-colloids
_composite materials
_computational materials science
_computer modeling
_computer simulation
_conducting polymers
_corrosion and oxidation
_corrosion protection
_crystal plasticity
_crystallization
_curing
_data analytics
_defects
_deformation
_deposition
_dielectrics
_diffraction, electron
_diffraction, neutron
_diffraction, X-ray (XRD)
_diffusion
_diodes
_dislocation dynamics
_dislocations
_drug delivery
_dye-sensitized solar cells (DSSCs)
_dysfunctional materials
_EBSD
_elastic properties
_electrical properties
_electrocatalysis
_electrochemistry
_electrode materials
_electron-beam melting
_electronic materials
_electronic properties
_electrospinning
_embrittlement
_energy harvesting
_epitactic or epitaxial growth
_fatigue
_FCC metals
_ferroelectrics
_FGMs
_fibers or fiber technology
_food colloids
_fracture
_fuel cells
_functional anisotropy
_functional materials
_gas-phase transport
_gelation
_geocomposites
_glass
_grain boundaries
_grain boundary engineering
_graphene
_graphitic carbon
_hardness
_HCP metals
_healing
_heat treatment
_hierarchical materials
_high entropy alloys
_high pressure torsion
_high throughput testing
_hot isostatic pressing
_hydrogels
_hydrogen storage or production
_hydrolysis
_II-VI compounds
_III-V compounds
_imaging
_In situ or operando
_infrared spectroscopy
_intercalation
_interfaces
_intermetallics
_ionomers
_kinetics
_laminates
_laser processing
_latticed effects
_layered materials
_light alloys
_light-emitting diodes
_liquid crystals
_lithography
_machining
_macro defects
_magnetic materials or properties
_magnetic ordering
_materials design
_materials for demanding environments
_materials for energy
_mechanical properties
_membranes
_mesoporous materials
_metal-insulator transition
_metal/organic frameworks (MOFs)
_metallic glasses
_metals
_metamaterials
_microanalysis
_microstructure
_minerals or mineralization
_molding
_molecular dynamics
_molecular simulation
_molecular-beam epitaxy (MBE)
_morphology
_multiferroics
_multilayers
_nanocomposites
_nanofunctionality
_nanoindentation
_nanolithography
_nanomaterials
_nanomedicines
_nanoporous materials
_natural materials
_NDT
_NMR
_nuclear materials
_nucleation
_omniphobic materials
_optical materials and properties
_organic electronics
_organic solar-cell materials
_permselective materials
_perovskite
_perovskite solar cell (PSCs)
_phase diagrams
_phase transformations
_phase-change materials (PCMs)
_phase-field modeling
_phosphors
_photocatalysis
_photonic materials
_photoreactive materials
_phototherapeutics
_photovoltaics (solar cells)
_piezoelectric materials
_plasma deposition
_plasmonic materials
_plating
_polymers
_porous materials
_powder technology
_pyroelectrics
_quasicrystals
_radiation damage
_radiation effects
_rapidly solidified materials
_redox flow batteries
_regenerative medicine
_resorbable materials
_responsive materials
_rheology
_sapphire/Al_2O_3
_scaffolds
_scanned-probe microcopy
_selective laser melting
_self-assembly
_self-healing materials
_SEM
_semiconductors
_sensing and sensors
_severe plastic deformation
_shape memory materials
_silicones
_singlet-exciton fission
_sintering
_small volume testing
_smart materials
_sodium-sulphur batteries
_soft interfaces
_soft matter
_sol-gel preparation
_solidification
_solvothermal/hydrothermal
_spectroscopy (XPS)
_spin glass
_spintronics
_sputter deposition
_STM
_superalloys
_supercapacitors
_superconductors
_superelasticity
_superhydrophobic
_surface treatments
_surfaces
_surfactants
_technical textiles
_TEM
_texture
_theranostics
_thermal barrier coatings
_thermal properties
_thermodynamics
_thermoelectrics
_thin-film or thick-film coatings
_TiO_2 rutile, anatase or brookite
_tissue engineering
_tomography
_topological insulators
_transparent conductors
_transport mechanisms
_tribology
_twinning
_TWIP steels
_two-photon adsorption
_UFG materials
_viscoelasticity
_viscosity
_water-splitting
_wear
_wood
_XPS
_zeolite

J Mater Sci

Thermo-migration behavior of SAC305 lead-free solder reinforced with fullerene nanoparticles

Guang Chen[1,2], Li Liu[2], Juan Du[2], Vadim V. Silberschmidt[2], Y. C. Chan[3], Changqing Liu[2,*], and Fengshun Wu[1,*]

[1] State Key Laboratory of Materials Processing and Die and Mould Technology, Huazhong University of Science and Technology, Wuhan 430074, China
[2] Wolfson School of Mechanical, Electrical and Manufacturing Engineering, Loughborough University, Loughborough, UK
[3] Department of Electronic Engineering, City University of Hong Kong, Tat Chee Avenue, Kowloon Tong, Hong Kong

Received: 18 April 2016
Accepted: 18 July 2016

ABSTRACT

In this work, SAC305 lead-free solder reinforced with 0.1 wt. % fullerene nanoparticles was prepared using a powder metallurgy method. A lab-made setup and a corresponding Cu/solder/Cu sample for thermo-migration (TM) test were designed and implemented. The feasibility of this setup for TM stressing was further verified with experimental and simulation methods; a temperature gradient in a solder seam was calculated as 1070 K/cm. Microstructural evolution and mechanical properties of both plain and composite solder alloys were then studied under the condition of TM stressing. It was shown that compared to unreinforced SAC305 solder, the process of diffusion of Cu atoms in the composite solder seam was remarkably suppressed. After the TM test for 600 h, Cu/solder interfaces in the composite solder seam were more stable and the inner structure remained more intact. Moreover, the addition of fullerene reinforcement can considerably affect a distribution of Cu_6Sn_5 formed as a result of dissolution of Cu atoms during the TM test. Hardness data across the solder seam were also found notably different because of the elemental redistribution caused by TM.

Introduction

SAC305 (wt. %) lead-free solder is widely used in electronic interconnections, thanks to its outstanding mechanical properties and good reliability under service conditions [1–3]. However, with fast developments in miniaturization and integration density in high-density electronic packages, electro- and thermo-migration (TM) failures induced by a high current density and large thermal gradients have become a main problem which would threaten the reliability of SAC305 solder interconnections [4–8]. The microstructural and mechanical evolution together with failure modes of solder joints under TM and EM stressing were also reported in previous studies [9–14]. Abdulhamid et al. [9] comprehensively

Address correspondence to E-mail: C.Liu@lboro.ac.uk; fengshunwu@hust.edu.cn

DOI 10.1007/s10853-016-0234-8

Journal : 10853 - Large 10853 | Dispatch : 21-7-2016 | Pages : 15
Article No. : 234 | LE | TYPESET
MS Code : JMSC-D-16-02130 | CP | DISK

investigated the damage mechanics of 95.5Sn4Ag 0.5Cu (SAC405) lead-free solder joints under TM stressing. After 1156 h TM stressing, they found that the Cu concentration in cold side is significantly higher than in hot side, while vacancy migration and Sn grain coarsening are in the opposing direction. In order to deeply understand the TM process, a fully coupled thermo-mechanical model is introduced by Basaran et al. [10]; the TM induced strength degradation and grain coarsening effects were both analyzed. Further, they also comparatively studied the migration mechanism in solder joints under EM and EM/TM stressing [12].It was also reported that TM is more likely to lead to failures of solder joints in some cases [15]. Therefore, with the trend of decreasing interconnection height, lead-free solder interconnections will face with reliability challenges related to electro-migration (EM) and in particular, TM.

According to previous studies, mechanical properties and solderability of existing lead-free solders could be improved by adding some foreign reinforcement (including metals, ceramics, and carbon-based materials) into a solder matrix to prepare a composite solder [16–21]. In addition, some researchers also attempted to investigate an effect of foreign reinforcement on EM in solder joints; it was reported that a suitable type and an appropriate amount of reinforcement added showed a positive effect on suppressing EM in solder joints [22–27]. However, to date, a systematic study of TM behavior of composite solder interconnections containing foreign reinforcement under large temperature gradient is still lacking.

As a zero-dimensional carbon-based nanomaterial, a unique molecular structure of fullerene determines its physical stability, low density as well as its excellent electrical, thermal, and mechanical properties [28–32]. Hence, it was usually used as reinforcing phase in preparing polymer- and metal-based composite materials [33, 34]. Chernogorova et al. [33] reported that tensile strength and microhardness of an aluminum/C60 composite alloy were significantly improved with the addition of C60 reinforcement. Watanabe et al. [34] fabricated an Mg–Al-Zn/fullerene (C60) composite alloy with a powder metallurgy method; the produced material demonstrated superelasticity under 548 K (with 256 % elongation). Our research group also prepared a SAC305/fullerene (mixture of C60 and C70) composite solder with a powder metallurgy method; the influence of fullerene on microstructure and mechanical properties on SAC solder joints were also systematically studied. It was found that addition of a proper amount of fullerene was effective in microstructural refinement and improvement in mechanical properties of solder joints [35]. To study further the effect of fullerene reinforcement on thermo-migration behavior of solder joints, in this paper, a SAC/fullerene composite solder reinforced with nano-sized fullerene particles was similarly prepared with the powder metallurgy method. Cu/Solder/Cu-structured interconnections were then formed for subsequent thermo-migration tests. It is widely reported that TM in Sn-based solder joints can be triggered when a temperature gradient and an environmental temperature reach at least 1000 K/cm and 100 °C, respectively [36]. Therefore, for TM tests, to achieve a large enough thermal gradient and environmental temperature without involving EM factor, a TM setup based on a heating plate with constant temperature and a Peltier thermoelectric cooler was designed and prepared. Feasibility of the as-designed setup and corresponding samples was also further verified in this work.

After progressively prolonged TM tests, evolution of interfacial intermetallics (IMCs) at the hot and cold ends and microstructure at the center of both plain and composite solder seams were comparatively studied. Additionally, the dissolution of Cu atoms into the solder seams was quantitatively evaluated. Moreover, the change in mechanical properties of the solder seams as a result of redistribution of elements during the TM test was also investigated. The findings in this work could promote our understanding of the impact of thermal gradient and environmental temperature on reliability of composite solder joints without the effect of current. It can also facilitate future studies on mitigating failures in solder joints induced by thermo-migration.

Experimental

Preparation of composite solder

SAC305 (wt. %) lead-free solder powder (with diameter of 25–45 μm, Beijing Compo, China) and a mixture of fullerene nanoparticles (approximately 80 % C60 and 20 % C70 with an average diameter of 30 nm, JCNANO Materials Tech, China) were utilized as original materials. For preparation of

Journal : 10853 - Large 10853 Dispatch : 21-7-2016 Pages : 15
Article No. : 234 LE TYPESET
MS Code : JMSC-D-16-02130 CP DISK

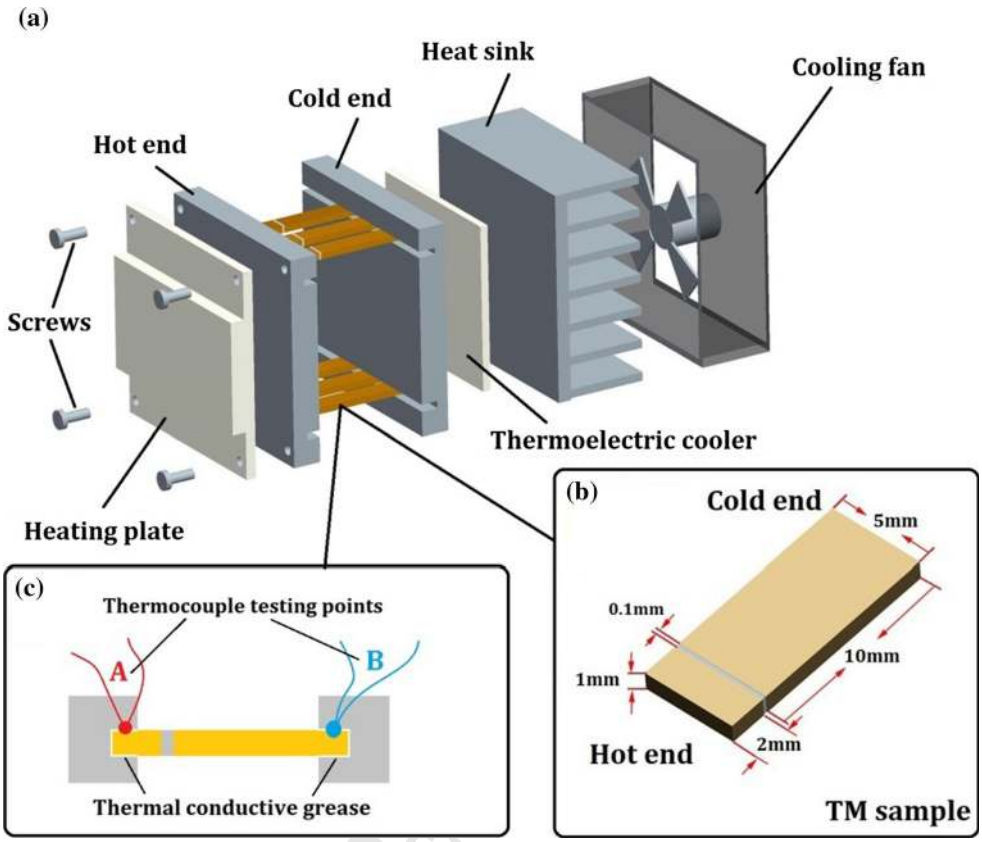

Figure 1 Schematic diagram of TM setup (**a**), TM samples (**b**), and thermocouple positions (**c**).

composite solder, the preweighted solder powder (99.9 wt %) and fullerene particles (0.1 wt. %) were homogenously blended in a planetary ball mill for 20 h. The mixed powder was then uniaxially compacted into solder billets (24 mm × 8 mm × 3 mm). These compacted solder billets were then sintered at 180 °C for 3 h in a vacuum sintering furnace before rolling into solder foils (with thickness of 100 μm) to prepare TM samples.

Design and preparation of TM setup and sample

To achieve a large enough thermal gradient across solder seams, a lab-made TM test setup was designed and prepared (as shown in Fig. 1a). The TM setup consisted of a constant-temperature heating plate with a temperature of 250 ± 5 °C as the heat resource and a Peltier thermoelectric cooler for cooling. A stable initial temperature (0 ± 2 °C) of the thermoelectric cooler was guaranteed by a temperature controller, while a heat sink and cooling fan were used to ensure its proper functioning during current stressing. The heating and cooling components were fixed on corresponding Cu bases with grooves (they were also the hot and cold sides in the TM tests). The spacing between two Cu bases was kept as 10 mm, while rectangular grooves with depth of 1 mm for placing TM samples were also produced on both hot and cold Cu bases with wire-electrode cutting. According to the difference of coefficients of heat conduction for different materials, the sample for TM was designed as an asymmetrical structure with a shorter hot end (2 mm) and a longer cold end (10 mm); a Cu plate (with thickness of 1 mm and width of 5 mm) was used as substrate material for both hot and cold sides of the sample. For sample preparation, end surfaces of the Cu substrates of both sides were well polished before soldering. A solder foil with dimensions of 5 mm × 1 mm × 0.1 mm was then clamped between two Cu substrates; finally, the clamped Cu substrates and the solder foil together with the clamp were placed in a reflow oven to prepare a sample of Cu/solder/Cu sandwich-like structure. The width of solder seams in reflowed solder samples remained similar to the thickness of the initial solder foils (namely, 100 μm); schematic diagram of a reflowed sample is shown in Fig. 1b. For

Journal : 10853 - Large 10853 Dispatch : 21-7-2016 Pages : 15
Article No. : 234 LE TYPESET
MS Code : JMSC-D-16-02130 CP DISK

the TM tests, the hot and cold ends of the prepared sample were correspondingly embedded in the above-mentioned grooves on both hot and cold Cu bases; the embedded depth was approximately 1 mm. To ensure good thermal conduction, thermal silicone grease was applied on each contact surface between different parts in the tests. In order to know the levels of temperature gradient and environmental temperature in the solder seam, experimental measurements and finite-element modeling were employed to evaluate the feasibility of the TM setup and the samples. A finite-element model was built with ANSYS 15.0 according to the actual dimensions of the setup and sample. To get good modeling results for a temperature distribution across the solder seam, thermocouples were first utilized to obtain the real temperature at points A and B during current stressing (the distances from A and B to the solder seam were 1 mm and 9 mm, respectively, as illustrated in Fig. 1c). The obtained average temperatures for points A and B were recorded when the temperature difference reached a balance; the recorded data were then set as the loading temperatures of the two ends for the subsequent modeling.

TM tests and characterization

In the TM tests, five samples for each kind of solder (plain and composite) were tested to satisfy different testing purposes. Specifically, microstructural evolution of one selected sample for each kind of solder was continuously observed a using scanning electron microscope (SEM QURTA 200) every 200 h; the total stressing time of the TM tests was designed as 600 h. The rest of samples that experienced the same TM stressing process were used for mechanical and compositional analysis. A focused ion beam (FIB) system was employed to study the distribution of Cu-Sn IMCs within a subsurface layer of the studied solder seams, while features of the inner structure were studied with an X-ray Micro-CT scanner (Metris XT H 160Xi) before and after the TM tests. Mechanical properties of the solder seams before and after the TM tests were also evaluated with a nanoindenter (Hysitron Ti750) at a constant load rate of 10 mN and a dwell time of 5 s. To know the difference in mechanical properties in different areas, in nanoindentation tests, each solder seam was evenly divided into three areas, denoted as A, B, and C at different positions between cold and hot ends. Five randomly selected locations for each area were tested to ensure reliability of the test results. In addition, to evaluate quantitatively the process of dissolution of Cu atoms into the solder seams under a large temperature gradient, the seams were cut off from the TM samples after different TM stressing times. After that, residual Cu at the surface of the solder seams was removed by fine polishing. The treated solder seams were then ultrasonically dissolved in aqua regia solution for elemental analysis using an inductively coupled plasma optical emission spectroscopy (ICP-OES, Varian-720) with test precision at PPM level.

Results and discussion

Feasibility evaluation of TM setup and sample

Evolution of measured temperature at points A and B with the stressing time in the TM test is shown in Fig. 2. It can be seen from the curves that the temperature saw a continual increase at the hot end after current stressing, while the temperature of the cold end demonstrated a small decrease first and then increased gradually; after approximately 7 min of the stressing, the temperature difference between the hot and cold ends reached equilibrium. During this stable stage, the average temperatures of the hot (point A) and cold (point B) ends were measured as 206.7 and 40.3 °C, respectively.

The temperature data obtained from the TM sample were used as original temperature parameter for finite-element modeling (FEM). The calculated temperature distributions in the TM setup and the solder seam are presented in Fig. 3. According to the simulation results, the temperature of hot side of the solder seam reached 181.4 °C, while the temperature of the cold side could reach 170.7 °C. In such a case, the temperature difference in the solder seam could achieve 1070 K/cm, since the width of the solder seam was 100 μm; the average environmental temperature at the solder seam was approximately 176 °C. According to previous studies [37], TM in lead-free solders can be triggered when the temperature gradient and the environmental temperature reach at least 1000 K/cm and 100 °C, respectively. In this work, it is clear that the obtained levels of temperature gradient and environmental temperature in the solder seam properly meet these requirements.

Journal : 10853 - Large 10853 Dispatch : 21-7-2016 Pages : 15
Article No. : 234 LE TYPESET
MS Code : JMSC-D-16-02130 CP DISK

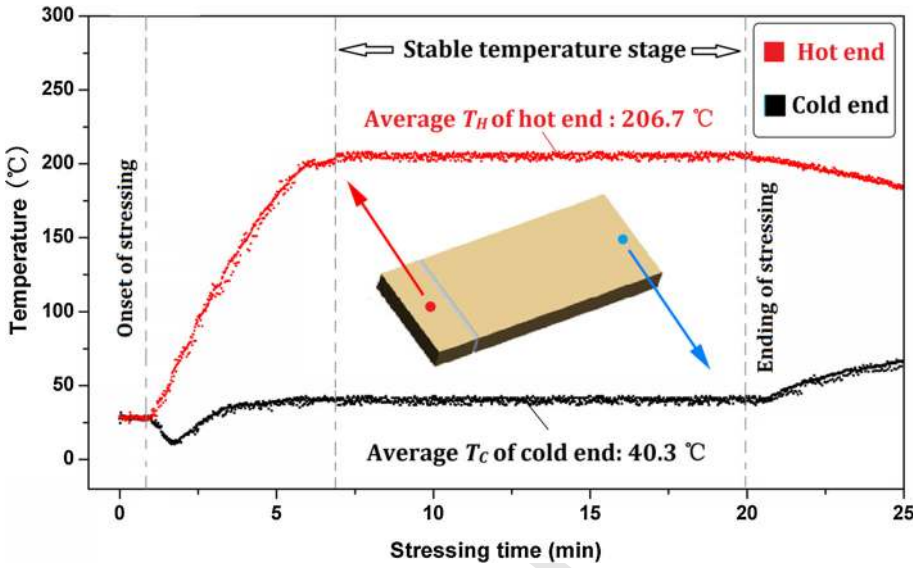

Figure 2 Evolution of temperature at points A and B with stressing time.

Thus, the TM setup and the produced sample are feasible for the TM tests.

Microstructural evolution

The microstructures of both plain and composite solder seams after different TM stressing times are shown in Figs. 4 and 5; the variation in thickness of interfacial Sn-Cu IMCs during TM testing is plotted in Fig. 6. It can be found from images of the solder seam before the TM test that β-Sn, Ag_3Sn IMC and Cu_6Sn_5 IMC were present in both kinds of solder seams. It is worth noting that the sizes of β-Sn phase and Ag_3Sn IMCs in the fullerene-reinforced composite solder seam were found to be apparently smaller than that in the plain SAC305 solder seam. This phenomenon can be explained in the following way: the added foreign reinforcement provided more nucleation sites during the solidification process; they also could impede the growth of grains by hindering atomic diffusion [35]. With the TM stressing time increasing, large quantities of bulky Cu-Sn IMCs can be found in both plain and composite solder seams; these Cu-Sn IMC are a mixture of the initial Cu_6Sn_5 in the SAC305 solder and the newly formed Cu_6Sn_5 as a result of dissolution and migration of Cu atoms coming from the Cu substrates. However, it is apparent that the size and quantity of these Cu-Sn IMCs in the plain SAC305 solder seam were larger than those in the composite solder seam, as shown in Figs. 4d, g, j and 5d, g, j. For the unreinforced SAC305 sample, it was found that Cu-Sn IMCs formed first at the hot end and the central position of the solder seam after 200 h stressing. With the stressing time increasing, the amount of Cu-Sn IMCs continued to grow, and these oval-shaped IMCs were also gradually distributed in the whole solder seam (after 400 h stressing). After 600 h TM stressing, most of the Cu-Sn IMCs were observed to locate at the central position and the cold end of the solder seam. By contrast, after 200 h TM stressing, although the formation and location of Cu-Sn IMCs in the fullerene-reinforced solder seam are similar to those in the plain solder seam, the size of these newly formed IMCs was clearly smaller when compared to their counterparts in the unreinforced SAC305 solder seam after the same stressing time. In addition, there is also a big difference in microstructures for two solder seams after 400 h and 600 h of TM stressing. Specifically, Cu-Sn IMCs formed as result of Cu diffusion were found in both solder seams at the early stressing stage (0–200 h); however, compared to the obvious migration of Cu-Sn IMCs in the plain solder seam, the changes of location of these IMCs in the composite solder seam were not that evident over time. Furthermore, most of IMCs in the composite solder seam were still located at the hot end and the central position after 400 h and 600 h stressing; only a small part of these IMCs were found at the position closed to the cold end, since the distribution of reinforcement added in the composite solder seam might not relatively uniform after reflow process.

In addition to the difference in microstructural evolution for two solder seams, the growth

Journal : 10853 - Large 10853 | Dispatch : 21-7-2016 | Pages : 15
Article No. : 234 | LE | TYPESET
MS Code : JMSC-D-16-02130 | CP | DISK

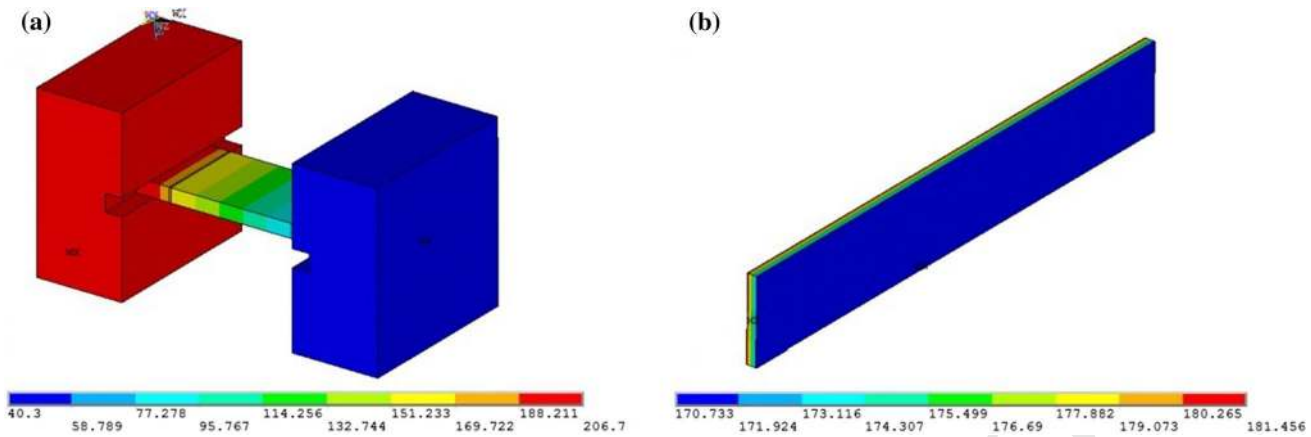

Figure 3 Temperature distributions in TM setup (**a**) and solder seam (**b**).

characteristics of interfacial IMCs of two types of samples were also different during TM stressing. For the plain solder seam, as shown in Fig. 4, the thickness of interfacial IMCs at the cold end obviously increased with the stressing time. The measured data for thickness shown in Fig. 6a also confirmed this trend; the thickness of interfacial IMCs at the cold end increased from the initial 2.12 μm to 8.96 μm after 600 h stressing, i.e., approximately 323 %. In addition, the morphological evolution of interfacial IMC at hot end also worth noting. It can also be found from Fig. 4 that the thickness of interfacial IMCs at the hot end similarly showed a gradually increasing trend during the first 400 h of stressing; the thickness increased from 2.51 μm to 3.36 μm, as shown in Fig. 6a. However, the thickness variation of interfacial IMC at hot end was not that pronounced compared to that for the cold end. Further, some Kirkendall voids were found in interfacial IMCs at the hot end after 400 h of TM stressing (see Fig. 4i). After 600 h of stressing, it can be seen that the initial interface at the hot end was damaged; only a very thin layer of IMC retained on the Cu substrate. The interfacial damage at the hot end can be attributed to considerable diffusion and migration of Cu atoms from the substrate into the solder seam during the TM stressing process; this interfacial damage also further blocked diffusion pathways for Cu atoms. As to the cold end, some granular Ag_3Sn phase with light gray color was also observed in Cu_6Sn_5 interfacial IMC after 600 h of TM stressing. The observed formation, migration, and location of Cu-Sn and Sn-Ag IMCs in the SAC305 solder seam during TM stressing illuminate that both Cu and Ag atoms migrate from the hot end to the cold one under the large temperature gradient; this finding in the present study is consistent with the current research results obtained by other researchers [15, 38].

In contrast, the growth of interfacial IMCs between the composite solder seam and the Cu substrates was mitigated considerably during TM stressing. Specifically, the thickness of interfacial IMCs at the cold end similarly showed an increase with the stressing time, from initial 1.86 to 4.86 μm after 600 h (Fig. 6b). The thickness increment for interfacial IMC at the cold end was approximately 161 %, significantly less than that in the plain SAC305 solder seam. In addition, no Ag_3Sn phase was found in interfacial IMCs at the cold end after 400 h or 600 h of TM stressing. For the hot end, the thickness of interfacial IMCs also increased with the stressing time, from initial 2.14 to 3.52 μm after 600 h. However, in contrast to serious damage happened at the hot interface in the plain SAC305 solder seam, morphology of interfacial IMCs at the hot end in the composite solder seam remained intact even after 600 h stressing, except that only a few of Kirkendall voids were found in this area. Thus, it is believed that incorporation of fullerene reinforcement inhibited the dissolution process of the Cu substrate, formation, and migration of Cu-Sn IMCs as well as the growth of interfacial IMCs. Based on the microstructural comparison between the plain and composite solder seams after TM stressing, the retardation of growth and migration of IMCs in the solder seam can be explained as follows. Fullerene is a nonreactive, noncoarsening material, when appearing in grain boundaries; present fullerene might hinder the migration of atoms

Journal : 10853 - Large 10853 | Dispatch : 21-7-2016 | Pages : 15
Article No. : 234 | LE | TYPESET
MS Code : JMSC-D-16-02130 | CP | DISK

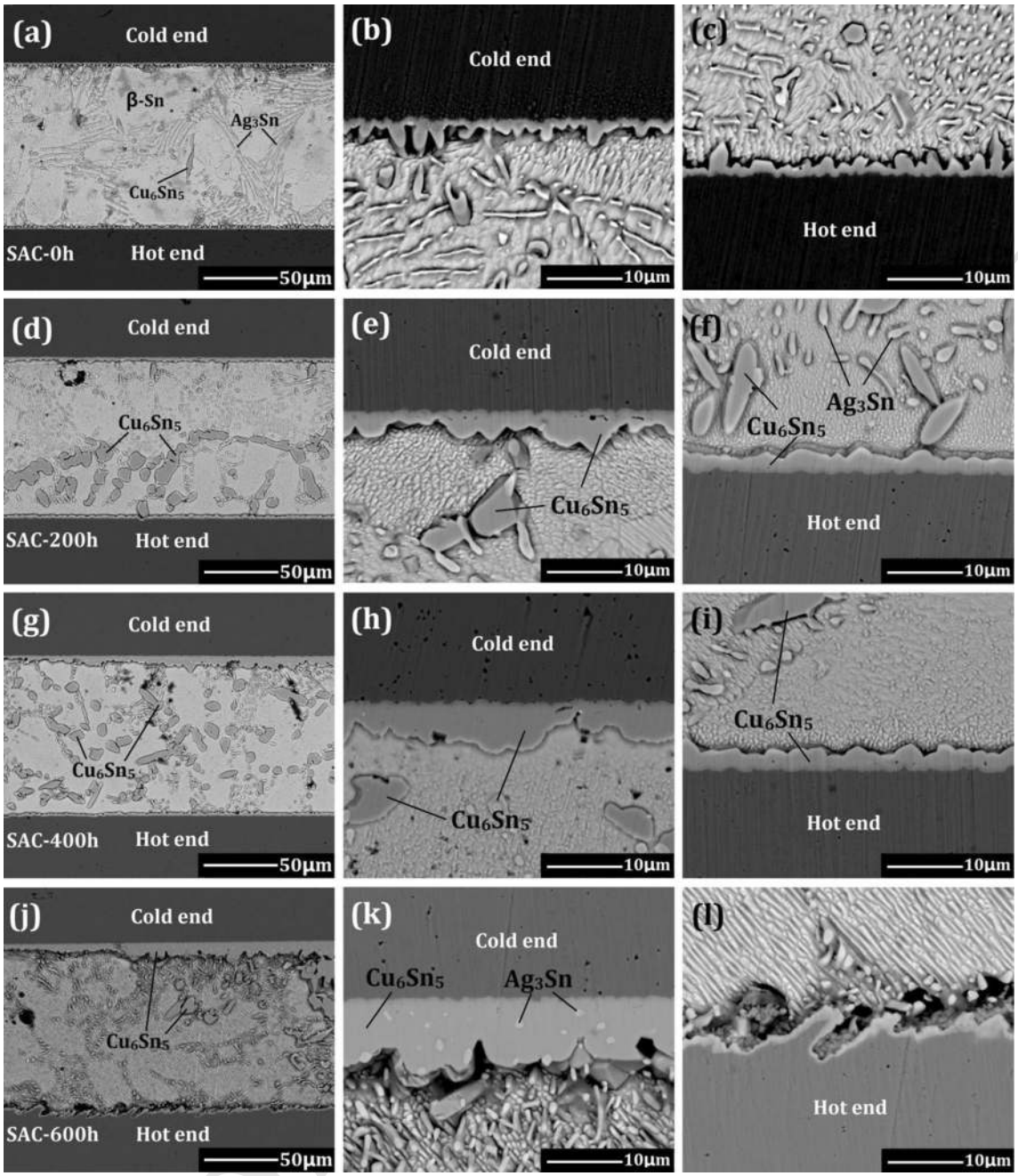

Figure 4 Microstructural evolution of SAC305 solder seam under temperature gradient of 1072 K/cm: **a**–**c** initial; **d**–**f** 200 h; **g**–**i** 400 h; **j**–**l** 600 h.

which could otherwise accelerate the process of IMC formation. Thus, the relationship between the growth rates for different crystal orientations of IMCs changed, leading to restrictions on growth and migration of IMCs. It is also widely believed that the diffusion coefficient of Cu atoms in the Sn matrix is relatively large [39]. Thus, combined diffusion between Cu and Sn atoms determined the growth of the interfacial Cu-Sn IMC phase at the solder/copper interface. According to our previous study on location of fullerene added in the solder matrix [35], it is supposed that some fullerene reinforcement stuck around the Cu-Sn phases, acting as barriers for diffusion of Sn to the Cu substrate or even obstructing formation of Cu_6Sn_5, inhibiting the growth of an interfacial IMC layer.

Journal : 10853 - Large 10853 Dispatch : 21-7-2016 Pages : 15
Article No. : 234 LE TYPESET
MS Code : JMSC-D-16-02130 CP DISK

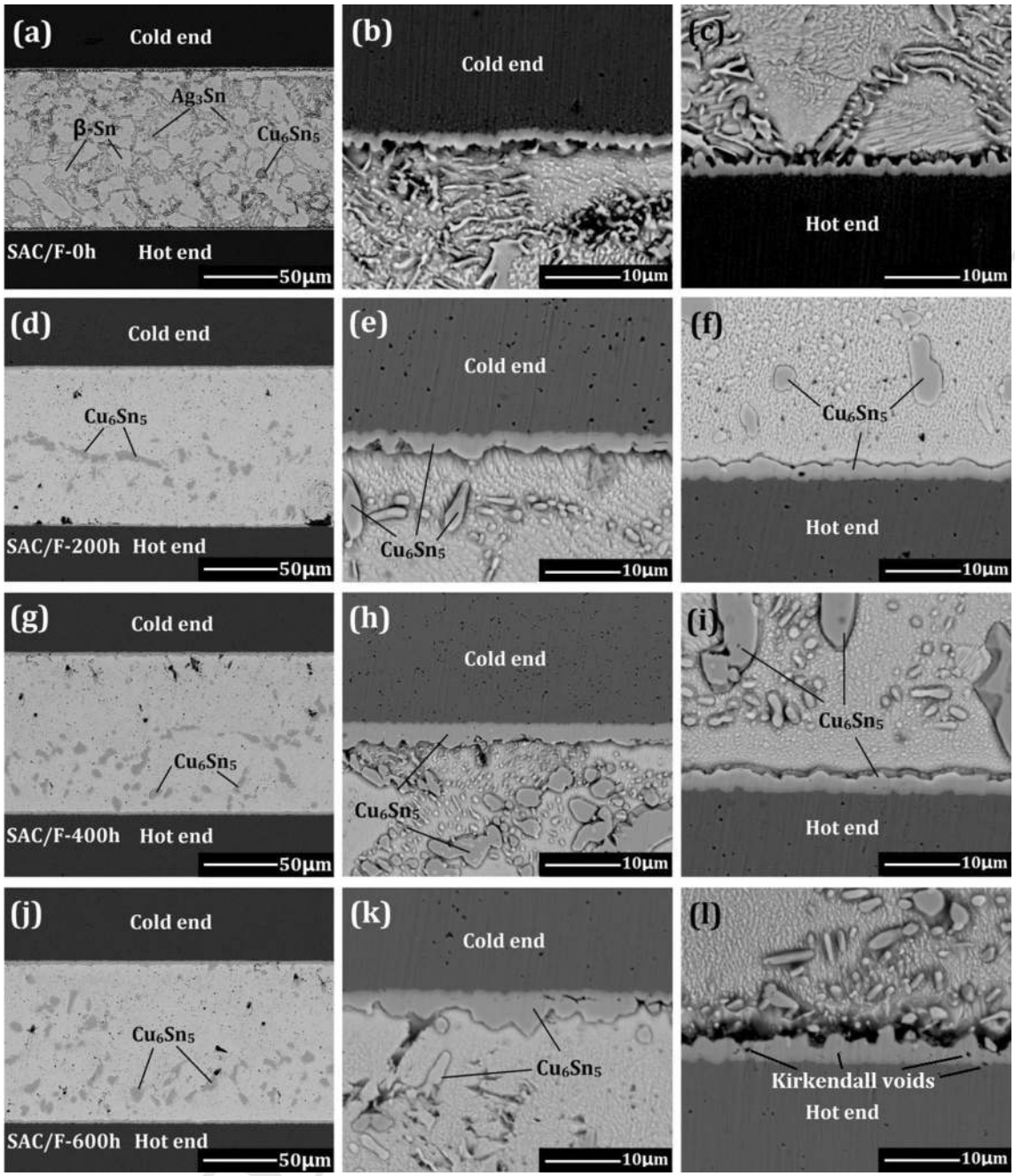

Figure 5 Microstructural evolution of SAC305/F composite solder seam under temperature gradient of 1072 K/cm: **a**–**c** original; **d**–**f** 200 h; **g**–**i** 400 h; **j**–**l** 600 h.

In addition, to understand further the distribution position of Cu-Sn IMCs in a subsurface layer of the solder seam, a dovetail groove with depth of 10 μm was prepared on the solder seams after 600 h of stressing using FIB, and the respective images are shown in Fig. 7. It can be known that after a long-term TM stressing, most of Cu-Sn IMCs formed by Cu diffusion were found to locate at the central position and the cold end of the plain SAC305 solder seam; the size and location of these IMCs were consistent with the SEM results as shown in Fig. 4. Similarly, the observed location and size of Cu-Sn IMCs in the composite solder seam using FIB were almost the same as the results shown in Fig. 5. The

Journal : 10853 - Large 10853 | Dispatch : 21-7-2016 | Pages : 15
Article No. : 234 | LE | TYPESET
MS Code : JMSC-D-16-02130 | CP | DISK

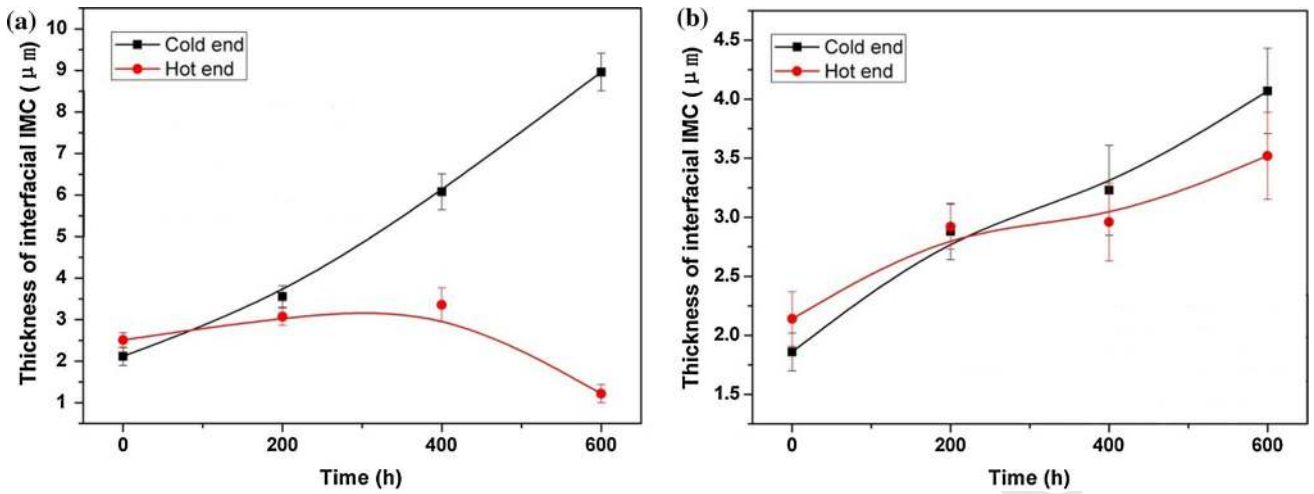

Figure 6 Evolution of thickness of Cu-Sn IMCs at the Cu/SAC305/Cu (**a**) and Cu/SAC305-F/Cu (**b**) with TM stressing time.

difference of location of Cu-Sn IMCs in the subsurface layer of two kinds for solder seams further indicates that the presence of foreign reinforcement can not only retard the migration of atoms on surface of the solder seam but also mitigate this diffusion in the inner of the solder seam.

To quantitatively measure the effect of addition of fullerene on diffusion of Cu atoms from the Cu substrate to the solder seams, the weight percentages of Cu in the solder seams were analyzed after different TM stressing times using ICP. For the ICP tests, in order to meet the testing requirements (the weight of sample is at least 100 mg) as well as to understand the Cu content as precise as possible, four treated samples (cut and polished solder seams; the weight of each solder seam was approximately 38 mg) were chosen for each kind of solder. The average Cu content for each solder was used as the testing result for comparative analysis; the ICP results are shown in Fig. 8. Although the cutting and polishing processes can cause errors in measuring the content of Cu in the solder seams, the obtained results shown in Fig. 8 revealed an obvious difference in the Cu content in two types of solder seams after different stressing times. Specifically, it increased with the TM stressing time; however, the increase rate in the plain SAC305 solder was much higher seam during whole stressing process than that in the composite solder seam. After 600 h of stressing, the average Cu content in the former reached 4.55 wt %, about 9 times higher than its initial value of 0.52 wt %. In contrast, the average Cu content in the composite solder seam after 600 h stressing was 2.09 wt %; only about 4 times higher than its initial value of 0.51 wt %. It is also worth noting that the increase rate of Cu in the plain SAC305 showed a decreasing trend in the interval from 400 h to 600 h. This phenomenon can also be explained by the fact that the diffusion and migration paths of Cu atoms at the Cu/solder interface were damaged due to a long-term TM stressing; this found change in the Cu content agrees well with the observed results as shown in Fig. 4. To avoid the error caused by the above-described phenomenon, only the data for times below 400 h were used to calculate the dissolution rate of Cu atoms during TM stressing. This rate was calculated employing the following formula:

$$v = \frac{M(w_2 - w_1)}{T}, \tag{1}$$

where v is the dissolution rate of Cu atoms, M is the average weight of the solder seam, T is the stressing time, w_1 and w_2 are the weight percentages of Cu in the solder seams after 0 h and 400 h stressing, respectively. After 400 h stressing, the net increase of Cu in the SAC305 solder seam was 3.27 wt %; since the weight of the solder seam was 38 mg, 1.24 mg of Cu was dissolved into the solder seam during 400 h of stressing. Due to the fact that the experimental parameters, including the temperature gradient and environmental temperature within the solder seam were relatively stable, the dissolution rate of Cu atoms form the substrate to the solder seam can thus be calculated as 3.1×10^{-6} g/h. By comparison, the increment of Cu content was only 0.488 mg in the composite solder seam after 400 h stressing; the

Journal : 10853 - Large 10853 Dispatch : 21-7-2016 Pages : 15
Article No. : 234 LE TYPESET
MS Code : JMSC-D-16-02130 CP DISK

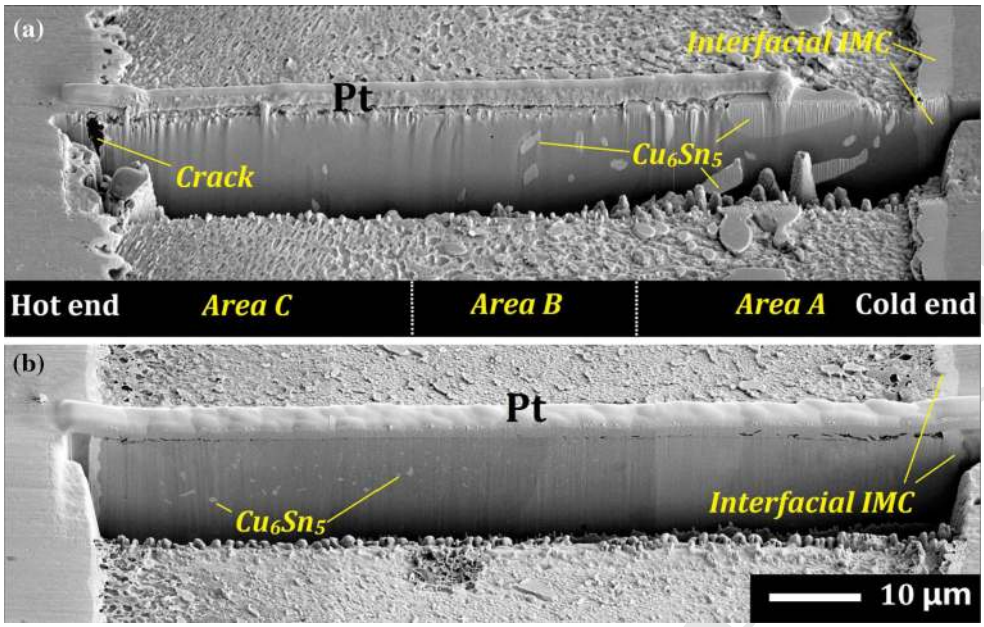

Figure 7 SEM images of FIB-cut trenches on subsurface layer of SAC305 (**a**) and SAC305/F (**b**) solder seams.

dissolution rate of Cu atoms was calculated as 1.22×10^{-6} g/h, which is only about a half of that in the plain solder seam. The ICP results and the calculated dissolution rates of Cu atoms clarify that addition of fullerene reinforcement contributed to mitigation of the diffusion from the Cu substrate into the solder seam under TM conditions.

To further access the effect of TM on inner structure of the solder seams, MCT nondestructive scanning was employed to analyze the solder seam area; the scanning results are shown in Fig. 9. Apparently, solder seam areas of both types of samples appear rather intact, without apparent defects before TM stressing (see Fig. 9a and c). However, big differences in inner structures were found for two solder seams after 600 h of TM stressing. Specifically, voids and cracks caused by elemental migration were found at both hot and cold interfaces of the plain SAC305 solder seam; further, large amounts of Cu-Sn IMCs (dark-gray areas) can also be observed at both sides of the solder seam (Fig. 9b). In contrast, the inner structure of the composite solder seam after long-term stressing seems to be less affected when compared with the SAC305 solder seam; only few voids were found. The newly formed Cu-Sn IMCs (dark-gray areas) are mainly distributed at the hot side of the solder seam, while only a small quantity of these IMCs were found at the cold side (Fig. 9d). The scanning results illustrate that addition of fullerene reinforcement into solder seam could help to maintain this structural integrity, extending the service life of solder interconnections exposed to a large temperature gradients.

Mechanical properties

In most previous studies, hardness of composite solder joints containing foreign reinforcements was evaluated using an automatic digital microhardness tester or a Vickers microhardness tester [11, 40–43]. Some researchers tested hardness and modulus of solder joints by employing a nanoindenter [44, 45]. By investigating hardness distribution in solder joints after current stressing, Ren et al. [46] reported that the hardness data showed a gradient distribution within a solder joint from an anode side to a cathode. However, by now, no studies mentioned the effect of thermal gradient on mechanical properties of composite solder joints containing foreign reinforcement. Therefore, in this investigation, to study the mechanical strength of small areas in solders seams, nanoindentor was used to assess a variation in hardness of different solder seams before and after 600 h TM stressing. A constant loading rate of 10 mN and a dwell time of 5 s were set as the operating parameters for these tests. Continuous monitoring of

Journal : 10853 - Large 10853 | Dispatch : 21-7-2016 | Pages : 15
Article No. : 234 | LE | TYPESET
MS Code : JMSC-D-16-02130 | CP | DISK

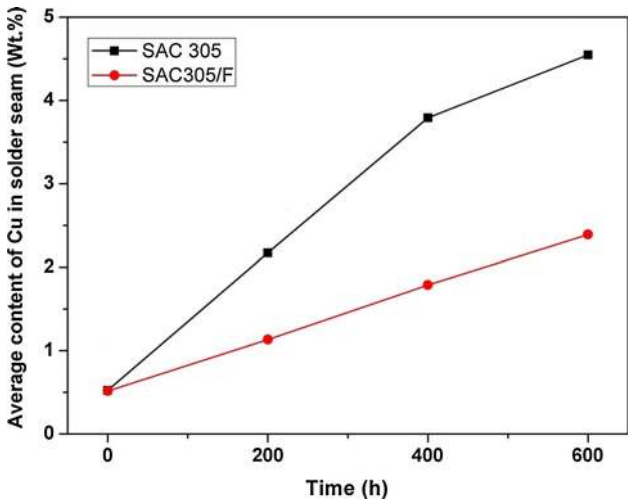

Figure 8 Evolution of weight percentage of Cu in solder seams with stressing time.

the constant applied load, constant dwell time, and indenter's depth displacement was applied to identify the hardness of different solder seams. In nanoindentation test, five points were randomly selected for both plain and composite solder seam before TM stressing. For the solder seams after 600 h stressing, as mentioned in the experimental part, five points were also randomly chosen from A, B, and C areas for each types of solder seams; the partitioning of areas A, B, and C is shown in Fig. 7.

All load–displacement diagrams for indentation points and the relevant hardness data for different samples are shown in Figs. 10 and ~~11~~. By comparing diagrams for the plain and composite solder seams before stressing, it is clear that the average indentation depth for the former (1338 nm) is larger than that for the later (1263 nm). This finding indicates that the resistance to deformation and hardness of the fullerene-reinforced composite solder were higher than those of the plain SAC305 solder. Improved mechanical strength can be explained as follows. On the one hand, the reduction in the maximum depth was due to the decrease in the grain sizes of the plain solder after doping with 0.1wt. % of fullerene nanoparticles (see Figs. 4a, 5a). On the other hand, a dispersion-strengthening effect as well as a pinning effect caused by introduction of foreign reinforcement also makes a considerable contribution. The calculated hardness data shown in ~~Fig. 11~~ also confirms this point of view; the average hardness of the fullerene-reinforced composite solder seam was 0.256 ± 0.05 GPa, which is 21.9 % higher than that of the plain SAC solder. However, it was found that a scatter in load–displacement diagrams for the composite solder seam was larger than that for the plain solder. This phenomenon indicates that the distribution of fullerene in the solder matrix might not be homogeneous. As well known, foreign reinforcement, especially, inert particles (including ceramics and carbon-based materials), are hard to be wetted reactively by the molten solder; there is a large interfacial free energy between the molten solder and the reinforcement. Thus, most of the added reinforcement might be excluded out of the molten solder during the soldering process, leading to a loss of reinforcement and inhomogeneous distributions of reinforcement in solder joints. This problem need to be further studied in the future to facilitate the application of composite solders in the electronic industry.

From Fig. 10b and d as well as the hardness data shown in Table 1, an obvious difference in indenter depths and distributions of hardness data can be found for the two studied types of TM stressed solder seams. These results vividly demonstrate that the hardness data of the plain SAC solder seam after 600 h stressing gradually decreased from its cold end (area A) to the hot end (area C), from the average value of 0.2534 GPa for area A to 0.1932 GPa for area C. This phenomenon can also be explained using migration and redistribution of different elements in the solder seam caused by TM stressing. During this process, a large amount of Cu atoms dissolved into the solder seam, forming Cu-Sn IMCs; these newly formed Cu-Sn IMCs were then continually pushed toward the cold end by the reverse thrust resulted from migration of Sn atoms from the cold end to the hot one [15]. In addition, like Cu atoms, Ag atoms were also confirmed to move in the same direction when the solders were subjected to a large temperature gradient. The migration and redistribution of Sn, Ag, and Cu during TM stressing would finally lead to an increase of Cu-Sn and Ag-Sn IMCs at the cold end and the central position of the solder seam. This point of view also agrees with the observed results as shown in Figs. 4 and 7a. The elemental redistribution caused by the temperature gradient would largely determine the hardness distribution in the solder seams. According to previous reports, the hardness values of the β-Sn, Ag_3Sn, and Cu_6Sn_5 phases are estimated as 0.35 ± 0.04 GPa [47], 2.9 ± 0.2 GPa [48], and 6.10 ± 0.53 GPa [49], respectively. It is apparent

Journal : 10853 - Large 10853 Dispatch : 21-7-2016 Pages : 15
Article No. : 234 LE TYPESET
MS Code : JMSC-D-16-02130 CP DISK

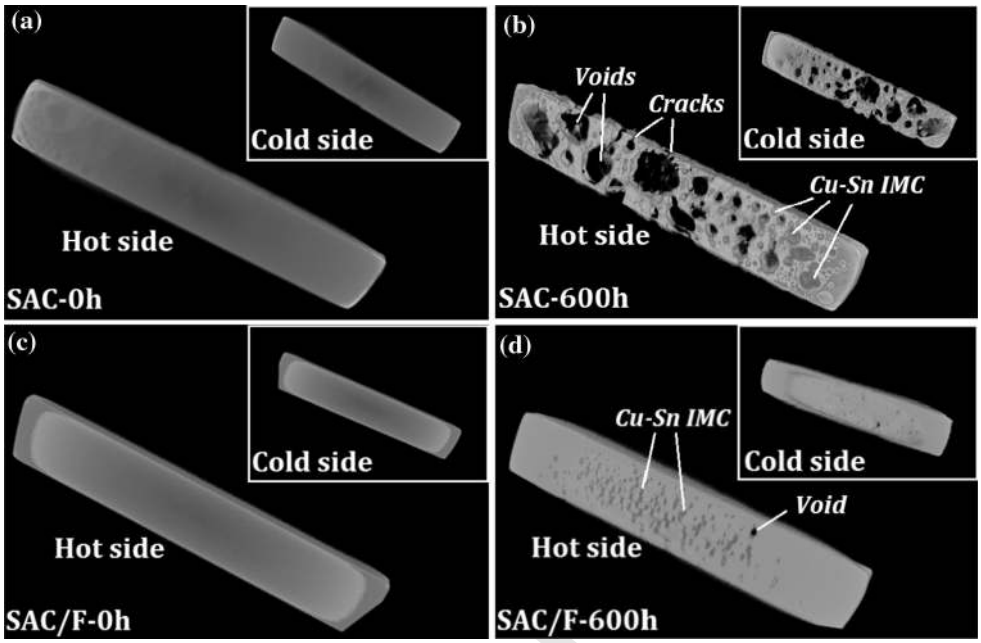

Figure 9 MCT scanning results for plain (**a**, **b**) and composite (**c**, **d**) solder seams before (**a**, **c**) and after (**b**, **d**) 600 h stressing.

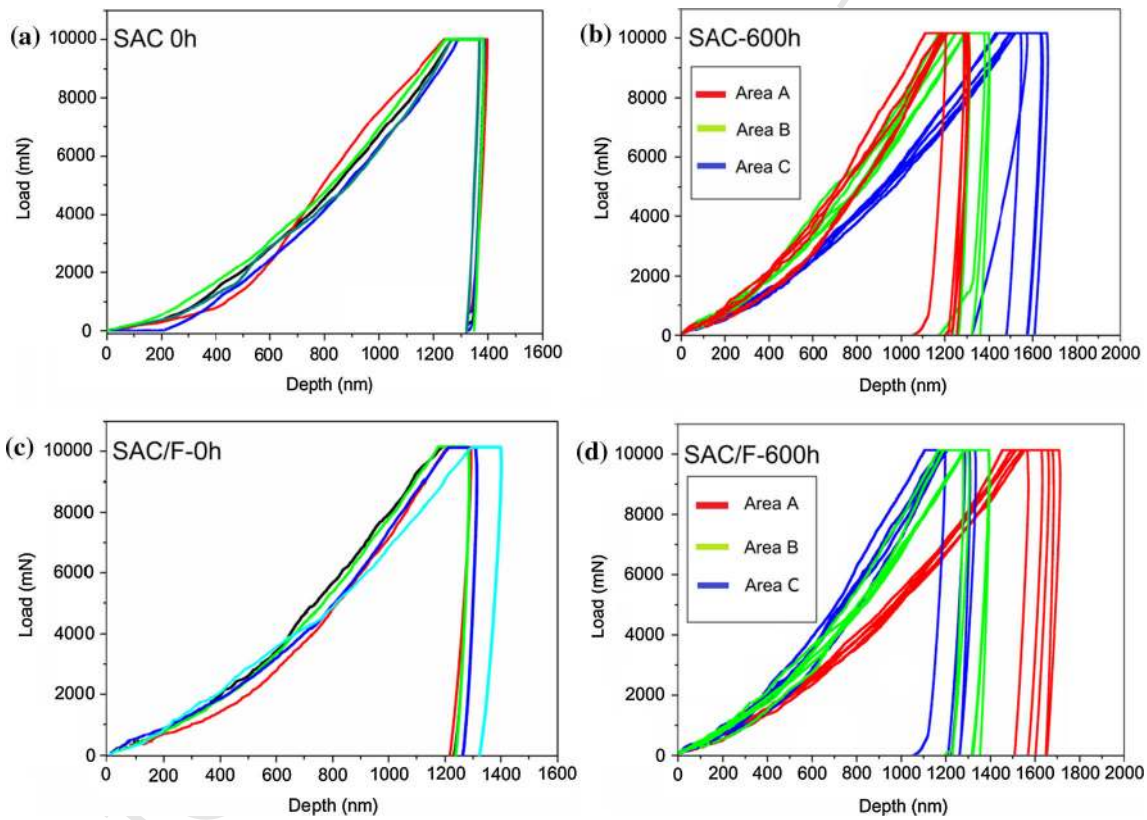

Figure 10 Testing results of indentation points for plain (**a**, **b**) and composite (**c**, **d**) solder seams before (**a**, **c**) and after (**b**, **d**) TM for 600 h.

that the enrichment of some rigid phase (including Cu-Sn and Ag- Sn IMCs) at the cold end gave a rise to an improvement of hardness in this area.

In contrast, the distribution of hardness values in the composite solder seam showed an opposite result: the hot end (area C) demonstrated a higher

Journal : 10853 - Large 10853 | Dispatch : 21-7-2016 | Pages : 15
Article No. : 234 | LE | TYPESET
MS Code : JMSC-D-16-02130 | CP | DISK

Table 1 Calculated hardness data for plain (a) and composite (b) solder seams before and after 600 h TM stressing

	Plain SAC solder (GPa)	Composite solder (GPa)
Reference Hardness (0 h)	0.2102	0.2562
Area A (600 h)	0.2534	0.2026
Area B (600 h)	0.212	0.2544
Area C (600 h)	0.1932	0.2634

hardness value than the cold end (area A). In consideration of the migration features of different elements as well as the obtained results shown in Figs. 5 and 7b, it can be concluded that the migration rate of all elements in the composite solder seam was diminished due to the addition of foreign reinforcement. As described in Sect. 3.2, most of the newly formed Cu-Sn IMCs were located at the central position and the hot end of the solder seam (namely, areas C and B); this was also the main reason for higher hardness values in these areas than in other areas. As for the cold end, although it was also exposed to a large temperature gradient during TM stressing, it was affected more like an isothermal aging process, since the migration rate of elements was largely mitigated. During the stressing period, the decline in hardness resulting from coarsening of the β-Sn and Ag_3Sn phases might exceed the enhancement effect caused by enrichment of Cu-Sn and Ag-Sn IMCs, leading to the overall decrease in hardness.

Conclusions

The SAC305/0.1F lead-free composite solder was produced through the powder metallurgy route. A temperature difference generator and relevant TM samples were designed and prepared; the evaluated temperature gradient in the solder seam in the setup was 1070 K/cm. After TM stressing, diffusion of Cu from the substrate to the solder seam was found in both plain and composite solders; this phenomenon was particularly prominent in the unreinforced solder seam. After 600 h of TM stressing, the interface at the hot end was damaged considerably, while a significant increase in the thickness was found in interfacial IMCs at the cold end. Although interfacial IMCs in the composite solder seam also showed an increasing trend during TM stressing, the interfacial structure remained intact compared with that of the plain solder seam. According to ICP results, the dissolution rate of Cu in the plain SAC305 solder under the employed experimental condition was 3.1×10^{-6} g/h; while for the composite solder, it was only 1.22×10^{-6} g/h. In addition, the scanning MCT results revealed that fullerene reinforcement helped to maintain integrity of the inner structure. The nanoindentation results demonstrated that hardness of the solder alloy obviously improved thanks to the doping of fullerene nanoparticles; moreover, mitigated elemental migration caused by the presence of the reinforcement could alter the distribution of hardness values in a solder seam under TM stressing. The findings of this study indicate that addition of fullerene could mitigate the negative effect of TM; hence, composite solders containing foreign reinforcement have a potential for a use under harsh service conditions.

Acknowledgements

The authors acknowledge research funding by the National Nature Science Foundation of China (NSFC) and The Research Grants Council (RGC) Joint Research project (NSFC No. 61261160498, RGC No.CityU101/12). This research was also supported by the China-European Union Technology Cooperation Project (No. 1110) as well as the Marie Curie International Research Staff Exchange Scheme Project within the 7th European Community Framework Programme, (No. PIRSES-GA-2010-269113). Thanks are also to the Analytical and Testing Centre at Huazhong University of Science Technology as well as LMCC at Loughborough University for their analytical and testing services.

Compliance with ethical standards

Conflict of Interest We declare that no conflict of interest exits in the present manuscript.

References

[1] Ervina EMN, Amares S, Yap TC (2013) A review: influence of nanoparticles reinforced on solder alloy. Solder Surf Mt Tech 25:229–241

Journal : 10853 - Large 10853 Dispatch : 21-7-2016 Pages : 15
Article No. : 234 LE TYPESET
MS Code : JMSC-D-16-02130 CP DISK

[2] Hu X, Chen W, Wu B (2012) Microstructure and tensile properties of Sn-1Cu lead-free solder alloy produced by directional solidification. Mater Sci Eng A 556:816–823

[3] Li Y, Moon K, Wong CP (2005) Electronics without lead. Science 308:1419–1420

[4] Basaran C, Abdulhamid MF (2009) Low temperature electromigration and thermomigration in lead-free solder joints. Mech Mater 41:1223–1241

[5] Chen C, Tong HM, Tu KN (2010) Electromigration and thermomigration in Pb-free flip-chip solder joints. Annu Rev Mater Res 40:531–555

[6] Ye H, Basaran C, Hopkins D (2003) Thermomigration in Pb-Sn solder joints under joule heating during electric current stressing. Appl Phys Lett 82:1045–1047

[7] Ye H, Basaran C, Hopkins D (2004) Mechanical implications of high current densities in flip chip solder joints. Int J Damage Mech 13:335–346

[8] Basaran C, Ye H, Hopkins D, Frear D, Lin JK (2005) Failure modes of flip chip solder joints under high electrical current density. Trans ASME J Elect Pack 127:157–163

[9] Abdulhamid M, Li S, Basaran C (2008) Thermomigration in lead-free solder joints. Int J Mater Struct Integ 2:11–34

[10] Basaran C, Li S, Abdulhamid M (2008) Thermomigration induced degradation in solder alloys. J Appl Phys 103:123520–123529

[11] Abdulhamid M, Basaran C (2009) Influence of thermomigration on lead-free solder joint mechanical properties. Trans ASME J Electr Pack 131:011002-1–01100212

[12] Abdulhamid M, Basaran C, Lai YS (2009) Thermomigration vs. electromigration in microelectronics solder joints. IEEE Trans Adv Packag 32:627–635

[13] Ma H (2009) Constitutive models of creep for lead-free solders. J Mater Sci 44:3841–3851

[14] Huang ML, Zhou Q, Zhao N, Liu XY, Zhang ZJ (2014) Reverse polarity effect and cross-solder interaction in Cu/Sn-9Zn/Ni interconnect during liquid-solid electromigration. J Mater Sci 49:1755–1763

[15] Chen C, Hsiao HY, Chang YW, Ouyang FY, Tu KN (2012) Thermomigration in solder joints. Mater Sci Eng R 73:85–100

[16] Gao LL, Xue SB, Zhang L, Sheng Z, Ji F, Dai W, Yu SL, Zeng G (2010) Effect of alloying elements on properties and microstructures of Sn-Ag-Cu solders. Microelectron Eng 87:2025–2034

[17] Wang CH, Li KT, Lin CY (2015) Minor Ga addition to effectively inhibit PdSn4 growth between Sn solder and Pd substrate. Intermetallics 67:102–110

[18] Han YD, Jing HY, Nai SML, Xu LY, Tan CM, Wei J (2012) Interfacial reaction and shear strength of Ni-coated carbon nanotubes reinforced Sn-Ag-Cu solder joints during thermal cycling. Intermetallics 31:72–78

[19] Sobhy M, El-Refai AM, Mousa MM, Saad G (2015) Effect of ageing time on the tensile behavior of Sn-3.5 wt% Ag-0.5 wt% Cu (SAC355) solder alloy with and without adding ZnO nanoparticles. Mater Sci Eng A 646:82–89

[20] Chellvarajoo S, Abdullah MZ, Samsudin Z (2015) Effects of Fe_2NiO_4 nanoparticles addition into lead free Sn-3.0Ag-0.5Cu solder pastes on microstructure and mechanical properties after reflow soldering process. Mater Des 67:197–208

[21] Tay SL, Haseeb ASMA, Johan MR, Munroe PR, Quadir MZ (2013) Influence of Ni nanoparticle on the morphology and growth of interfacial intermetallic compounds between Sne3.8Age0.7Cu lead-free solder and copper substrate. Intermetallics 33:8–15

[22] Ma LM, Xu GG, Sun J, Guo F, Wang XT (2011) Effects of co additions on electromigration behaviors in Sn–3.0 Ag–0.5 Cu-based solder joint. J Mater Sci 46:4896–4905

[23] Bashir MN, Haseeb ASMA, Rahman AZMS, Fazal MA, Kao CR (2015) Reduction of electromigration damage in SAC305 solder joints by adding Ni nanoparticles through flux doping. J Mater Sci 46:6748–6756

[24] He HW, Xu GC, Guo F (2009) Effect of small amount of rare earth addition on electromigration in eutectic SnBi solder reaction couple. J Mater Sci 44:2089–2096

[25] Zhao R, Ma LM, Zuo Y, Liu SH, Guo F (2013) Retarding electromigration in lead-free solder joints by alloying and composite approaches. J Electron Mater 42:280–287

[26] Hu X, Chan YC, Zhang KL, Yung KC (2013) Effect of graphene doping on microstructural and mechanical properties of Sn–8Zn–3Bi solder joints together with electromigration analysis. J Alloy Compd 580:162–171

[27] Guo F, Xu G, He H (2009) Electromigration behaviors in Sb particle-reinforced composite eutectic SnAgCu solder joints. J Mater Sci 44:5595–5601

[28] Wang FD, Jin C, Liang H, Tang Y, Zhang H, Yang YJ (2014) Effects of fullerene C60 nanoparticles on A549 cells. Environ Toxicol Phar 37:656–661

[29] Li H, Tee BCK, Cha JJ, Cui Y, Chung JW, Lee SY, Bao Z (2012) High-mobility field effect transistors from large-area solution-grown aligned C60 single crystals. J Am Chem Soc 134:2760–2765

[30] John P, Harris F (1999) Carbon nanotubes and related structures. Cambridge University Press, Cambridge

[31] Calvert P (1999) Nanotube composites: a recipe for strength. Nature 399:210–211

[32] Komatsu K, Murata M, Murata Y (2005) Encapsulation of molecular hydrogen in fullerene C60 by organic synthesis. Science 307:238–240

[33] Chernogorova O, Drozdova E, Ovchinnikova I, Soldatov AV, Ekimov E (2012) Structure and properties of superelastic

Journal : 10853 - Large 10853 | Dispatch : 21-7-2016 | Pages : 15
Article No. : 234 | LE | TYPESET
MS Code : JMSC-D-16-02130 | CP | DISK

hard carbon phase created in fullerene-metal composites by high temperature-high pressure treatment. J Appl Phys 111:112601–112605

[34] Watanabe H, Fukusumi M, Ishikawa K, Shimizu T (2006) Superplasticity in a fullerene-dispersed Mg–Al–Zn alloy composite. Scripta Mater 54:1575–1580

[35] Chen G, Wu FS, Liu C, Xia W, Liu H (2015) Effects of fullerenes reinforcement on the performance of 96.5Sn–3Ag–0.5Cu lead-free solder. Mater Sci Eng A 636:484–492

[36] Huang AT, Gusak AM, Tu KN, Lai YS (2006) Thermomigration in SnPb composite flip chip solder joints. Appl Phys Lett 88:141911–141913

[37] Ouyang FY, Kao CL (2011) In situ observation of thermomigration of Sn atoms to the hot end of 96.5Sn-3Ag-0.5Cu flip chip solder joints. J Appl Phys 110:123525–123529

[38] Huntington HB (1973) In: Aaronson HI (ed) Diffusion, american society for metals. OH, Metals Park

[39] Chang CW, Yang SC, Tu CT, Kao CR (2007) Cross-interaction between Ni and Cu across Sn layers with different thickness. J Electron Mater 36:1455–1461

[40] Tang Y, Li GY, Pan YC (2014) Effects of TiO_2 nanoparticles addition on microstructure, microhardness and tensile properties of Sn–3.0Ag–0.5Cu–xTiO_2 composite solder. Mater Des 55:574–582

[41] Gain AK, Chan YC, Yung WKC (2011) Microstructure, thermal analysis and hardness of a Sn–Ag–Cu–1 wt% nano-TiO_2 composite solder on flexible ball grid array substrates. Microelectron Reliab 51:975–984

[42] Ping L, Pei Y, Jim L (2008) Effect of SiC nanoparticle additions on microstructure and microhardness of Sn–Ag–Cu solder alloy. J Electron Mater 37:874–879

[43] Chuang TH, Tsao LC, Chung CH, Chang SY (2012) Evolution of Ag3Sn compounds and microhardness of Sn3.5Ag0.5Cu nano-composite solders during different cooling rate and aging. Mater Des 39:475–483

[44] Chellvarajoo S, Abdullah MZ, Khor CY (2015) Effects of diamond nanoparticles reinforcement into lead-free Sn–3.0Ag–0.5Cu solder pastes on microstructure and mechanical properties after reflow soldering process. Mater Des 82:206–215

[45] Yang Z, Zhou W, Wu P (2014) Effects of Ni-coated carbon nanotubes addition on the microstructure and mechanical properties of Sn–Ag–Cu solder alloys. Mater Sci Eng, A 590:295–300

[46] Ren F, Xu LH, Zhang X, Pang HL, Tu KN (2006) In-Situ Study of the Effect of electromigration on strain evolution and mechanical property change in lead-free solder joints, 56th Electronic Components and Technology Conference, San Diego, 2006. pp. 0569–5503

[47] Sadiq M, Lecomte JS, Cherkaoui M (2013) Nanoindentation for measuring individual phase mechanical properties of Sn-Ag-Cu lead-free solders incorporating pileup effects. Chaotic Model and Simul 2:335–348

[48] Chromik RR, Vinci RP, Allen SL, Notis MR (2003) Nanoindentation measurements on Cu–Sn and Ag–Sn intermetallics formed in Pb-free solder joints. J Mater Res 18:2251–2261

[49] Jang GY, Lee JW, Duh JG (2004) The nanoindentation characteristics of Cu_6Sn_5, Cu_3Sn, and Ni_3Sn_4 intermetallic compounds in the solder bump. J Electron Mater 33:1103–1110

Journal : 10853 - Large 10853 | Dispatch : 21-7-2016 | Pages : 15
Article No. : 234 | ☐ LE | ☐ TYPESET
MS Code : JMSC-D-16-02130 | ☑ CP | ☑ DISK

Journal : **10853**
Article : **234**

Springer
the language of science

Author Query Form

Please ensure you fill out your response to the queries raised below and return this form along with your corrections

Dear Author

During the process of typesetting your article, the following queries have arisen. Please check your typeset proof carefully against the queries listed below and mark the necessary changes either directly on the proof/online grid or in the 'Author's response' area provided below

Query	Details Required	Author's Response
AQ1	Figure 11 had been cited in the text, but not provided, kindly check and amend the changes.	
AQ2	Please check the edits made in the article title and amend if necessary.	